COMPREHENSIVE REVIEW OF NANOPOROUS ANODIC ALUMINA: SYNTHESIS STRATEGIES AND FUTURE PERSPECTIVES

Article history
Received
17th January 2025
Revised
14th March 2025
Accepted
4th June 2025
Published
1st December 2025

Ao Wang[ab], Nur Dalilah Johari[ac], Abdul Hakim Md Yusop[ac], Muhamad Azizi Bin Mat Yajid[ac], Wan Fahmin Faiz Wan Ali[ac*]

[a]Faculty of Mechanical Engineering, Universiti Teknologi Malaysia, 81310 UTM Johor Bahru, Malaysia.
[b]College of Physics and Electronic Engineering, Hebei Minzu Normal University, Chengde, Hebei Province, 067000 China.
[c]Materials Research Consultancy Group, Universiti Teknologi Malaysia, 81310 UTM Johor Bahru, Malaysia.

[*]Corresponding email: wan_fahmin@utm.my

ABSTRACT

Nanoporous anodised aluminium (NAA) is a valuable substance characterised by a uniform pore structure, exceptional chemical stability, and robust mechanical qualities. It possesses extensive applicability in biology, energy, sensing, and optics. This research initially examines the historical development of NAA, elucidates the fundamental principles of its formation process, and elucidates the mechanism underlying its distinctive structure. This study systematically analyses the impact of key parameters—oxidation voltage, oxidation temperature, electrolyte type, and concentration—on the anodization process and their effects on the structural characteristics of NAA, including pore size, pore spacing, and oxide film thickness. The comparison of outcomes from various preparation circumstances elucidates the approach for optimising the procedure to get the desired structure. This research delineates the unique applications of NAA in the biomedical domain, encompassing drug carriers, tissue engineering, and antibacterial coatings, while also categorising its use in energy conversion and storage, including osmotic energy conversion and battery augmentation. The advanced developments of NAA in humidity, gas, and optical sensors are thoroughly examined, particularly their potential applications in the creation of photonic crystals, photocatalysis, and random laser platforms. This article anticipates the future trajectory of NAA, identifies its technical challenges and research priorities concerning large-scale preparation, precise structural control, and multifunctional applications, and offers a theoretical foundation and practical guidance for further investigation in this domain.

Keywords: *nanoporous anodic aluminium, electrochemistry, nanotechnology.*

© 2025 Penerbit UTM Press. All rights reserved

1.0 INTRODUCTION

Nanotechnology promotes the development of materials through precise control of nanoscale structures, creating new features and functions, improving performance, and extensive innovation in application fields, covering various materials with specific structures and properties, such as nanoparticles, nanowires, and nanofilms. Alumina nanofilms have the advantages of high-temperature stability, chemical inertness, and electrical insulation. Nanoporous alumina prepared by anodic oxidation, also known as

NAA, has been studied extensively among many materials, and its advantages include an adjustable pore structure and high surface area [1]. The emergence of nanotechnology has enabled the application of NAA in a wide range of fields. These include data storage [2], development of chemical or biological sensor devices [3], template-assisted fabrication of nanostructures [4], and fabrication of corrosion-resistant materials [5]. All these applications require NAA to have appropriate structural and chemical properties, which requires adjusting the technical parameters of the anodizing process, pre-treatment, and post-treatment.

Therefore, this paper systematically reviews the synthesis characteristics of NAA and its synthesis process in different electrolytes (oxalic acid, sulfuric acid, and phosphoric acid), focusing on the effects of key parameters, such as oxidation voltage, temperature, and electrolyte type, on the structure and performance of NAA. In addition, based on the research progress in recent years, this article discusses an environmentally friendly synthesis method of NAA under the concept of green chemistry, as well as its emerging applications in sensors, energy storage, biomedicine, and other fields. Finally, this article looks forward to the future research direction of NAA, emphasizes the importance of composite functionalization and sustainable development, and provides a critical perspective for further enhancing the multifunctional applications of NAA.

2.0 OVERVIEW OF NANOPOROUS ANODIZED ALUMINA (NAA)

2.1 Development of NAA

Anodic oxidation has been used as a method to prevent the corrosion of aluminium and its alloys by forming a dense oxide layer on the surface of aluminium. With the deepening of research, scientists have begun to explore the preparation of structured anodized aluminium with micron-sized pores by controlling electrolysis conditions, which provides a potential platform for applications such as adsorption, catalysis, and sensing. Subsequently, the introduction of nanotechnology led to the further evolution of anodic aluminium oxide (AAO) in the study of NAA, providing new opportunities for innovation in the fields of nanotemplates [6,7], sensors [8,9], and biomedicine [10,11]. This section outlines the development of the NAA anodization process.

Anodization is used to prevent [7] the corrosion of aluminium and its alloys by forming a dense oxide layer on the aluminium surface. In 1875, French scientist Eugene Ducretet first reported the passivation of aluminium through chemical reactions. He observed changes in the surface color of aluminium when polarized in an aqueous medium and described the formation of aluminium oxide owing to the interaction between aluminium and oxygen [12]. Subsequently, German scientist Charles Pollak developed the first electrochemical apparatus for anodization, studying the properties of the anodic oxides formed in different electrolytes. The results demonstrated that anodization can enhance the corrosion resistance of aluminium and its alloys for industrial applications [13]. With the advancement of research, scientists have begun exploring ways to fabricate structured anodized aluminium with micron-scale pores by controlling electrolytic conditions. These structures provide a promising platform for adsorption, catalysis, and sensing applications. Later, the introduction of nanotechnology led to the evolution of anodized aluminium oxide (AAO) into nanoporous anodized aluminium (NAA), offering new opportunities for innovations in nanostructured templates, sensors, and biomedical fields [6]. This section provides an overview of the development of the NAA anodization processes.

In the late 1940s, British researcher Simon Wernick [14] first introduced the term "anodization" to define the electrochemical oxidation of aluminium, marking the formal adoption of this concept in both industrial and academic contexts. In the early 1950s, Keller et al. [15] used scanning electron microscopy (SEM) to characterize NAA and observed its

ordered nanoporous structure. They proposed a schematic model, known as the KHR model, to explain the formation of NAA. In the 1970s, O'Sullivan and Wood [16,17] introduced the field-assisted dissolution (FAD) model. This model explains pore nucleation as a result of the enhanced dissolution of aluminium oxide by acidic electrolytes, driven by localized field concentrations. Thirty years later, Baron-Wiechec et al. [18] proposed a new theory called the field-assisted plasticity (FAP) model. The FAP model attributes pore formation primarily to the non-uniform migration of cations and anions within the anodized aluminium oxide layer during oxidation, with the electric field driving the pore initiation and growth. Although both theories are widely accepted and supported by experimental evidence, they are fundamentally contradictory. Both the models rely heavily on the role of the electrolyte in the anodization process. Consequently, the exact mechanism underlying the formation of the porous anodic layers remains a topic of active scientific debate.

2.2 Basic Principles

Aluminium (Al) and oxygen (O) have very strong chemical affinities, so they can easily become alumina (Al_2O_3). Even if Al is only exposed to air, a thin oxide film of 10 Å can be formed on its surface. This oxide film is also called 'natural oxide film'. However, owing to its very thin oxide layer, it is difficult to utilize it as an anti-corrosion protective coating. As the anode, the aluminium sample was electrolyzed in a certain electrolyte, and an oxide film was formed on the surface of the Al. This is known as 'aluminium anodic oxidation' electrolysis [19]. The type of electrolyte, temperature, and applied current or voltage are critical factors that influence the ultimate chemical and physical properties of the anode layer. The film is formed by the migration of Al^{3+} cations in the Al and OH^- and O^{2-} anions under a high electric field [16]. The anodic reaction for the overall film growth is equation (1):

$$2Al_{(sol)} + 3H_2O_{(liq)} \rightarrow Al_2O_{3(ox)} + 3H_{2(g)} \quad (1)$$

The oxide films can be divided into barrier oxide layers (BOL) and porous oxide layers (POL), as depicted in Figure 1. In one situation, only dense BOL with thicknesses of a few hundred nanometres (nm) will be produced. In another situation, there is a combination of a BOL with a thickness between 10 and 100 nm and a POL up to10 μm in thickness [16]. In BOL, especially in alkaline electrolytes, H^+ and OH^- generated by the water-splitting reaction are neutralized locally by the reaction of equation (2). In contrast, in the POL, H^+ can locally dissolve more oxides as equation (3):

$$2H^+(aq) + OH^-(aq) \rightarrow H_2O(l) \quad (2)$$

$$1/2Al_2O_3(s) + 3H^+(aq) \rightarrow Al^{3+}(aq) + 3/2H_2O(l) \quad (3)$$

The pores in the POL result from the material flowing from the barrier layers below the pore base to the cell wall regions [10]. It is worth noting that these subjects have been studied for many years, and researchers continue to investigate the mechanisms of NAA production in depth. In the following section, we outline the important findings regarding the fabrication of NAA.

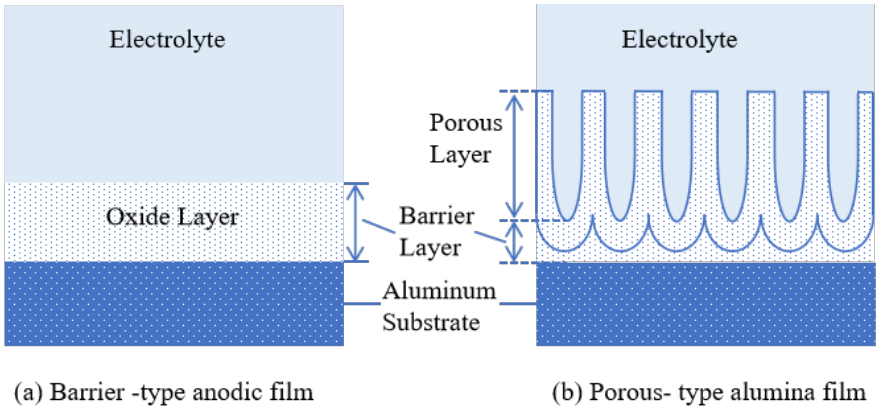

Figure 1: Schematic representation of (a) a barrier-type anodic film and (b) a porous-type alumina film.

The manufacture and applications of nanoporous anodised aluminium (NAA) have advanced significantly, although certain obstacles remain. The current state of anodising technology limits large-scale industrial uses by balancing cost-effectiveness, manufacturing scalability, and structural precision. It is still difficult to achieve accurate tunability on various scales, even though apertures, distribution, and shape can be somewhat adjusted [20]. To improve the scalability and usability of NAA in a range of cutting-edge technologies, future research should concentrate on establishing cost-effective high-yield production techniques, optimising anode technology, and incorporating multi-scale structural design.

3.0 SYNTHESIS OF NANOPOROUS ANODIC ALUMINA (NAA)

3.1 Synthesis Process

The preparation of aluminium oxide thin films by the electrochemical method was first proposed by Keller et al. (1953); however, this method is rough, time-consuming, and has a low repetition rate [15]. Masuda and Fukuda [21] later proposed a two-step anodic oxidation method to prepare NAA with stable pore formation and a high repetition rate. In addition, researchers have invented a series of manufacturing methods according to actual needs, such as multistep anodization [22], nanoimprint lithography anodization [18], and pulse anodization [24]. There are benefits and drawbacks to each anodising technique. Due to its high pore structure regularity and good reproducibility, the two-step anodising procedure is extensively employed; however, it involves a number of processes and takes a long time to prepare. The pore structure can be further optimised using a multi-step anodising procedure, although the expense and complexity of the process are increased. Although it requires costly lithography templates, the nanoimprint lithography anodising approach allows for exact pore organisation and dimensional control. By varying the applied voltage pulse, the pulse anodization method may precisely control the aperture and pore spacing; nevertheless, it necessitates precise process parameter optimisation. Owing to the widespread use of two-step anodizing, many other improved anodizing methods are optimized based on this principle. Therefore, this study introduces a two-step anodic oxidation in detail. The specific process is illustrated (Figure 2).

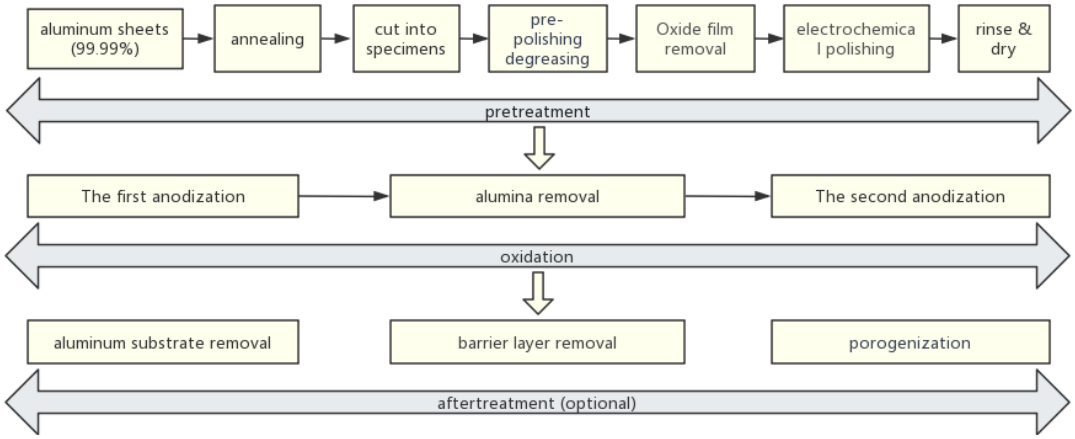

Figure 2: The synthetization flow of nanoporous anodized alumina (NAA).

3.2 Different Parameters of Anodic Oxidation

The structural properties of NAA are affected by various process parameters during anodization and the properties of the substrate [25]. These factors are briefly described in this section.

3.2.1 The Effects of Oxidation Voltage

The voltage has a direct effect on the inherent porosity of the anode layer; a lower voltage creates a large number of very small pores, whereas a higher voltage produces few large pores, which tends to favor the production of a thicker dense layer [26]. This relationship can be expressed by the following equation (4):

$$d_{pore} = C_{pore} \times \Delta V \quad (4)$$

where d_{pore} is the pore diameter, C_{pore} is a proportionality constant that is approximately equal to 1.3 nm/V, and ΔV is the anodic oxidation voltage. In addition, the application of a gradual voltage can affect the morphology of NAA. Put et al. [27] showed that the anodic film morphology and oxide formation efficiency depend on the voltage change in the electrolyte. A sudden decrease in voltage (approximately 50 % change drop) produces a distinct boundary between fine and rough regions in the thin-film morphology, whereas a sudden increase in voltage does not. Furthermore, the voltage also has a significant impact on the spacing and width of the pores, although anodization in a high electric field results in burned oxides [28]. One et al. [22-24] measured the breakdown voltage and obtained breakdown voltages corresponding to commonly used electrolytes (oxalic acid, phosphoric acid, and sulfuric acid) as 50 V, 197 V, and 27 V, respectively. The voltages corresponding to the best sequence are 40 V, 195 V, 25 V which are slight below the breakdown voltage; therefore, precise voltage control is required. It is also worth noting that excessive voltage could cause electronic breakdown, which manifests as the breakdown of the aluminium foil.

3.2.2 The Effects of Oxidation Temperature

The effect of temperature on NAA was mainly reflected in the pore spacing and degree of ordering. Leszek et al. [30] reported the effect of temperature on the pore spacing in a phosphoric acid electrolyte. It was concluded that the hole spacing increases with increasing temperature, with an experimental value of 0.02-0.32 nm/°C. In 2018, Li et al. [31] explored the order degree of NAA template over a wide temperature range (5-50 °C).

They believe that the degree of order of NAA templates increases first and then decreases when the temperature rises, and 15 °C is the ideal temperature for the degree of order in oxalic acid electrolyte. Leontiev et al. [32] studied the effect of temperature change during anodization with 0.3 M oxalic acid. When anodizing aluminium at a voltage of 40 V, increasing the temperature (0-40 °C) of the electrolyte increases the contribution of diffusion current. When the thickness of the NAA film reaches a particular value (50 μm), the increase in the diffusion current may cause non-uniformity of the oxide layer, destroying the ordered arrangement of the hexagonal pores. The order of the pores did not change with temperature for a sufficiently thin (~10 μm) NAA layer produced at the same voltage.

3.2.3 The Effects of Electrolyte

The electrolyte played a vital role in the formation of NAA, which directly determined the pore distance (D_{int}). Three common electrolytes have been used in NAA.

Oxalic acid.
Ramana Reddy et al. [33] investigated the structure of NAA films by increasing the electrolyte molarity from 0.1 M to 0.9 M at 8 °C while keeping the anodic oxidation potential at 40 V. The results showed that the regularity of the NAA film changed with electrolyte concentration, with the NAA film formed at 0.3 M having the highest regularity. Self-ordered alumina nanopores (D_{int} = 100 nm) were produced in a 0.3 M oxalic acid solution (40 V) using a standard mild anodization (MA) method [34]. Huang et al. [35] reported a high-field anodization process for the manufacture of NAA in high-concentration oxalic acid (0.75 M), and a highly ordered NAA structure was rapidly fabricated using a two-step anodization process. At this higher concentration and higher temperature (30 °C) oxalic acid solution, stable high-field anodization can be achieved without breakdown owing to the thinner barrier layer. After 50 min of oxidation, NAA with a thickness of approximately 57 nm, pore spacing of approximately 120 nm, and pore diameter of approximately 75 nm were obtained. The temperature of oxalic acid can improve the regularity of the NAA structure, but too high a temperature (>40 °C) can cause the pores to collapse. The reaction mechanism for oxalic acid is shown in equation (5).

$$HC_2O_4^-(aq) \rightarrow C_2O_4^{2-}(oxide) + H^+(aq) \quad (5)$$

Sulfuric acid.
Sulfuric acid anodization is effective at relatively low voltages (15-40 V) and produces porous oxide films with small pore diameters [36]. In a typical mild anodization (MA) process, self-ordered alumina nanopores (D_{int} = 63 nm) were obtained in 0.3 M sulfuric acid solution (25 V) [36]. Bruera et al. [37] performed highly ordered NAA under two conditions: (a). 0.3 M sulfuric acid electrolytes (20 V, 10 °C), and (b). 2 M sulfuric acid electrolyte (15 V, 5 °C). The results showed three important trends: (a). The pore diameter and pore distance are proportional to the voltage (b). The density of the pores decreased with increasing voltage, and (c). The thickness of the oxide film increases with the electrolyte concentration, temperature, and anodizing voltage. Sulka et al. [22] investigated a three-step oxidation process in sulfuric acid electrolyte at various voltages. The findings revealed that the nearly flawlessly ordered aluminium honeycomb structure was primarily created during the second-phase anodic oxidation process at 15–25 V. It is also worth noting that the three-step anodization process has no discernible effect on the order and size of the pores. The reaction mechanism in sulfuric acid is given by equation (6).

$$HSO_4^-(aq) \rightarrow SO_4^{2-}(oxide) + H^+(aq) \quad (6)$$

Phosphoric acid.

In a typical mild anodization (MA) process, self-ordered alumina nanopores (D_{int} = 500 nm) were obtained in 0.1 M phosphoric acid solution when the anodization voltage exceeded 180 V and approached 195 V at 0°C [38]. However, the process required 16 h to complete. Sadasivan et al. [39] produced NAA in one-step anodic oxidation using 0.53 M phosphoric acid at a voltage range of 40-120 V, yielding pore diameters in the 60-200 nm range. Jagminien et al. [40] also reported this method in the same year, in which NAA was prepared by one-step anodic oxidation in 0.4 M phosphoric acid at a voltage of 80 V at 25°C. The pore size obtained was 80 nm, and the pore distance was 208 nm. The reaction mechanism of phosphoric acid is shown in equation (7).

$$H_2PO_4^-(aq) \rightarrow HPO_4^{2-}(oxide) + H^+(aq) \quad (7)$$

Table 1 summarizes the NAA with various anodization parameters. Based on the summary, it can be observed that different electrolytes exhibit their own advantages and disadvantages throughout the anodization process. The ability of oxalic acid to produce a nanopore structure with a reasonable pore size and ordered arrangement makes it a popular electrolyte. However, a lengthy anodization period is necessary for the electrolysis of oxalic acid [33]. In contrast, sulphuric acid electrolyte has the ability to quickly create high-density small-pore nanopore structures, which greatly benefits it in applications requiring a high specific surface area. It should be mentioned, nonetheless, that the sulphuric acid system is vulnerable to an excessively high rate of oxidation during prolonged anodization, which could result in a reduction in the stability of the nanopore structure [36]. Phosphoric acid electrolytes tend to form large pore size structures, which is conducive to achieving high porosity. However, it is often difficult to obtain a uniform nanopore structure and requires the application of a higher operating voltage [39]. Therefore, in practical applications, the selection of electrolytes requires comprehensive consideration of the characteristics of the target pore structure (such as pore size, porosity, pore density), anodizing efficiency, and structural uniformity, and trade-offs and optimizations between these parameters.

Table 1: The summary of fabrication conditions and results of nanoporous anodic alumina in three common acids.

	Oxidation method	Concentration (M)	Voltage (V)	Temperature (°C)	Pore diameter (nm)	Pore distance (nm)	Ref.
Oxalic acid	1-step	0.3	40	1	-	95	[36]
	2-step	0.3	40	0, 20, 40	79±3, 65±5, 58±1	101±6, 99±8, 95±9	[32]
	2-step	0.3	120	0, 10, 20	69±1, 68±1, 59±1	281±23, 272±19, 295±20	[32]
	1-step	0.2	40	28	40	103	[40]
	2-step	0.75	50	30	75	120	[35]
Sulfuric acid	1-step	0.3	25	10	-	60.0	[36]
	2-step	0.3	10, 15, 20	10	21.0, 27.8, 34.0	29.9, 40.9, 56	[37]
	2-step	0.3	10, 15, 20	20	21.4, 27.3, 34.2	29.9, 42.1, 51.9	[37]
	2-step	0.3	10, 15, 20	30	21.2, 26.3, 29.7	31.3, 42.3, 49.9	[37]
	2-step	2	10, 12, 15	5	15.8, 19.9, 20.4	26.5, 30.9, 34.7	[37]
	2-step	2	10, 12, 15	10	18.4, 19.9, 22.4	28.6, 30.2, 35.5	[37]
	2-step	2	10, 12, 15	20	18.2, 17.9, 23.2	28.1, 32.7, 37.2	[37]
	1-step	1.53	15	18	13.5	40.5	[40]

Phosphoric acid	2-step	0.3	195	0	-	500	[38]
	1-step	0.4	80	25	80	208	[40]
	1-step	0.53	120, 80, 40	-	200, 100, 60	-	[39]
	1-step	10 wt %	160	3	-	420	[36]

4.0 APPLICATIONS OF NAA

Nanoporous anodic aluminium oxide (NAA) has emerged as a prominent material in contemporary scientific studies because of its distinctive nanostructure and superior physical and chemical properties. As a multifunctional platform created through anodization, NAA exhibits significant versatility in both structural and functional designs. By regulating critical parameters, including pore size, porosity, and thickness, NAA demonstrates enhanced mechanical strength and chemical stability, while also enabling precise functional modulation at the nanoscale. These attributes have facilitated extensive research and applications of NAA in biology, energy, sensing, and optics, demonstrating significant developmental potential. Subsequently, we concentrate on the most recent advancements in the study and application outcomes of NAA in these domains, elucidating its distinctive performance and technological significance.

4.1 Biomedical Applications

NAA, a biocompatible material, has demonstrated significant potential in the biomedical sector. Kapruwan et al. [41] established a novel platform utilizing nanoporous anodized aluminium photonic crystals (NAA-GIF) for real-time assessment of drug molecule release kinetics. NAA-GIF was synthesized through sequential pulse anodization (SPA) in an oxalic acid electrolyte solution to create a photonic crystal structure featuring two photonic band gaps (PSBs), with the first PSB coinciding with the absorption band of the drug molecule and the second PSB situated outside the absorption range. The experimental and numerical simulation findings indicate that the relative concentration of the medication within the pore can be precisely monitored using the reflectance spectrum of NAA-GIF. In later investigations, scientists developed a novel hybrid NAA-GIF by integrating SPA and constant potential anodization technology, with SPA modulation at the top and a linear pore channel at the bottom, to investigate the loading and release dynamics of doxorubicin. This research indicated that the drip approach could more precisely forecast the nanopore filling process. A model study utilizing two inverse exponential decay functions indicated that the drug release quantity within the pore is time-dependent, substantially influenced by pore length and flow rate, and can be regulated through diffusion. This technology facilitates the effective real-time characterization of drug release and provides novel technological assistance for the design and development of drug delivery systems. Lednický and Bonyár [42] proposed a technique for fabricating ordered arrays of AuNPs on epoxy substrates. Gold nanoparticles were synthesized on nanobowl-shaped aluminium templates using a solid-state annealing technique, which was created by selective chemical etching of porous anodic aluminium oxide (PAA) developed on aluminium plates via a controlled anodization process. This technique facilitates precise regulation of the dimensions, morphology, and interparticle distance of nanoparticles across extensive areas (several square centimetres), thus enhancing their localized surface plasmon resonance (LSPR) and surface-enhanced Raman scattering (SERS) spectral characteristics within the range of 535–625 nm. Following the transfer of gold nanoparticles to the epoxy substrate, they were selectively etched to create epoxy nanopillar structures topped with flat disc-shaped gold nanoparticles. This nanocomposite demonstrated a bulk refractive index sensitivity ranging from 83 to

108 nm RIU^{-1}. Label-free DNA detection was accomplished in sensing studies by identifying Giardia lamblia-specific DNA sequences (20 bp).

After 2 h of hybridization with 1 μM target DNA, the LSPR absorption spectrum exhibited a redshift of 6.6 nm, and the limit of detection (LOD) was approximately 5 nM. This AuNP/polymer-based plasmonic sensor is one of the inaugural sensors used to effectively accomplish label-free DNA detection, offering a novel technical trajectory for biosensing. Pla et al. [43] introduced an innovative hybrid sensor utilizing aptamer-gated nanomaterials for the rapid and effective detection of Staphylococcus aureus. The technique employs nanoporous anodic aluminium oxide (NAA) as a scaffold, incorporates the fluorescent indicator rhodamine B, and occludes pores with designated aptamers. The aptamer can specifically identify Staphylococcus aureus cells and occlude the pores to prevent the release of the fluorophore. In the presence of the target bacterium, the aptamer was displaced by the bacteria, resulting in pore opening and subsequent release of the fluorophore. The sensor has a detection range of 2–5 CFU mL^{-1} for bacterial concentrations (with lower limits in buffer and blood) and can be finalized in less than 1 h. The approach was evaluated using 25 clinical samples, and the results exhibited a high degree of consistency with typical hospital reference technology. In contrast to conventional approaches, the sensor is sensitive, quick, cost-effective, and does not require intricate procedures, such as polymerase chain reaction (PCR), rendering it highly ideal for on-site rapid detection systems. Agbe et al. [44] applied a silver–polymethylhydrosiloxane (PMHS) coating to the surface of NAA. The synthesized Ag-PMHS nanocomposite demonstrated remarkable antibacterial efficacy against clinically significant planktonic bacteria, yielding inhibition zone measurements of 25.3 ± 0.5 mm for Pseudomonas aeruginosa (PA) (Gramme −ve), 24.8 ± 0.5 mm for Escherichia coli (E. coli) (Gramme −ve), and 23.3 ± 3.6 mm for Staphylococcus aureus (SA) (Gramme +ve), with adhesion reduction rates of 99.0%, 99.5%, and 99.3%, respectively. The Ag-PMHS nanocomposite coating on anodized aluminium exhibited superior antibacterial and anti-biofouling characteristics.

4.2 Energy Applications

Nanoporous anodized aluminium (NAA) has extensive potential applications in the energy sector owing to its distinctive nanostructure and multifunctional characteristics. In recent years, researchers have employed NAA's revolutionary applications in osmotic energy conversion and passive radiation cooling technology to provide novel concepts and methods for efficient energy utilization. NAA serves as a cost-effective and efficient nanofluid platform for the conversion of osmotic energy through reverse electrodialysis (RED). Liu et al. [45] employed a straightforward in situ growth approach to create a light-responsive sub-nanochannel of the metal-organic framework (MOF) NH_2-MIL-53, encapsulating spiropyran (SP-MIL-53) using an NAA membrane as a template. This channel may be opened and closed, thereby efficiently regulating ion flux and functioning as a sophisticated ion gate. Under ultraviolet irradiation, the on-off ratio in a 10 mM potassium chloride aqueous solution reached 16.2, offering an efficient approach for harnessing salinity gradient energy. Chen et al. [46] presented a hybrid membrane that incorporated a hydrogel within a nanofluid matrix. A generator utilizing this novel hybrid membrane demonstrated exceptional energy conversion efficiency and mechanical characteristics. The distinctive nanochannels and negatively charged regions inside the hybrid membrane confer significant cation selectivity, with a peak power density of 11.72 W/m^2 under a 500-fold salinity gradient.

Passive radiative cooling technology is an efficient method for reducing the energy usage in cooling systems. NAA nanostructures demonstrated their capacity for daytime cooling in 2019, exhibiting a solar reflectivity ($\overline{R_{sol}}$) of 94%, an IR emittance ($\overline{\varepsilon_{IR}}$)of 90%, a cooling power (P_{cool}) of 64 W/m^2, and a temperature drop (ΔT) of 2.6 °C [47]. We clarify how the morphological characteristics and chemical composition of NAA-Al

samples influence their optical properties and cooling efficiencies. The thickness of the alumina layer, variation in pore spacing and porosity, and counterions employed substantially influenced the cooling capability of the NAA-Al structures. Díaz-Lobo et al. [48] enhanced prior research by recording a maximum temperature reduction ΔT of 8.0 °C under direct sunlight on a summer day in Spain and determined a peak cooling power P_{cool} of 175 W/m^2 for NAA-Al samples anodized in sulfuric acid, exhibiting a thickness of 12 μm and a porosity of 10%.

4.3 Sensors Applications

NAA-based sensors are classified into two categories: electrical and optical. NAA-based electrical sensors primarily fall into two categories: capacitance and resistance. A thin metallic coating is typically applied to the surface of the NAA to serve as an electrode for humidity measurement [49]. Yang et al. [50] developed two distinct substrates, silicon and anodized aluminum oxide (NAA), for the manufacture of relative humidity sensors to enhance sensitivity. The capacitive response of indium nitride compound-doped oxygen sensors (InN:O) utilizing NAA substrates surpassed that of InN:O sensors employing silicon substrates. The magnetic field influences the response recovery time of the NAA humidity sensors. Chung et al. [51] discovered that a magnetic field can markedly improve the efficacy of anodized aluminium oxide (NAA) humidity sensors across various acid concentrations and relative humidity (RH) levels. At low relative humidity (45%), the magnetic field enhances the capacitive response of the sensor by promoting a more organized arrangement of water molecules. Conversely, at high relative humidity (> 45%), the capacitance of NAA sensors subjected to a magnetic field exhibits a notable enhancement, attributable to the phonon-assisted electron tunnelling mechanism and the increased conductivity of the pore walls. The results demonstrated that the application of a magnetic field can significantly improve the sensitivity and stability of the NAA humidity sensor across a broad relative humidity range.

Optical sensors transform the interaction between a substrate and analyte into optical signals. This technology is extensively utilized in chemical trace detection owing to its advantages, including being label-free, fast, and non-invasive. NAA serves as an exceptional substrate for diverse optical sensing devices, offering benefits such as nanoscale pores, self-assembly characteristics, programmable geometry, and favourable biocompatibility [49]. Malinovskis et al. [52] synthesized oriented ZnO nanorods exhibiting photoluminescence properties and incorporated them into a two-step vertical NAA structure. The analyte, human vascular endothelial growth factor, was identified by diminishing the PL intensity via ZnO nanorods. Surface plasmon resonance (SPR) denotes the oscillation of electrons on a metal surface induced by the incoming light. The analyte is identified by alterations in the SPR absorbance of the substrate [49]. Lednický et al. [42] identified unlabelled DNA from Giardia lamblia by assessing the red shift in the LSPR absorbance spectrum induced by gold nanoparticles fabricated on a nanobowl barrier on an aluminium substrate, following the removal of the NAA layer.

4.4 Optical and Photonic Applications

Nanoporous anodic aluminium oxide (NAA), a multifunctional medium produced by electrochemical aluminium oxidation, has extensive applications in the optical domain. Its meticulously engineered nanoporous framework may create diverse photonic crystal (PC) structures and utilize numerous interactions between light and matter (such as Bragg diffraction, confinement, and interference) to attain the exacting control of light. NAA-PC can be integrated with luminescent materials to modulate the characteristics of the emitted light across the spectrum and is extensively utilized in the construction of luminescence and quantum optical systems. Owing to the ongoing advancements in anodization

techniques and photonic crystal architectures, NAA has demonstrated significant potential in optical domains including telecommunications, sensing, imaging, energy, and laser systems, while also encountering challenges and opportunities for further optimization and expansion [53]. Liu et al. [54] introduced a novel photonic crystal consisting of nanoporous anodic aluminium oxide (NAA) broadband distributed Bragg reflector (BDBR) functionalized with titanium dioxide (TiO_2) for photocatalysis driven by visible light. NAA-BDBR, produced by double exponential pulse anodization (DEPA) technology, has an extensive photon stop band (PSB) characterized by high resolution and spectral tunability, with its width adjustable from 70 ± 6 to 153 ± 9 nm (in air). The photocatalytic efficacy of TiO_2-NAA-BDBR with variable PSB widths under visible-NIR irradiation was examined by three model photodegradation reactions of organic substances with absorption bands located in the visible light spectrum. The photocatalytic efficiency is maximized when the red edge of the PSB aligns closely with the electronic band gap of the TiO_2 coating, a shift of the red edge towards the visible spectrum results in a substantial decline in photocatalytic performance. Nonetheless, when the red edge of the PSB coincides with the absorption band of the organic materials, the photocatalytic efficiency is restored.

This indicates that TiO_2-BDBR can augment the photocatalytic reaction by decelerating the group velocity of photons within a certain spectral range, offering a novel concept for the development of high-performance photocatalysts. Li et al. [55] fabricated multiband-responsive NAA-based photonic crystals (PCs) using pulsed anodization. These PCs demonstrate several photonic band gaps (PBGs) in the visible to near-infrared (vis-NIR) spectrum, enabling accurate experimental manipulation of the positions of these band gaps. Physical vapor deposition (PVD) applied a silver layer onto the surface of an NAA-based photonic crystal to modify its refractive index, successfully creating a uniform distributed Bragg reflector (DBR) structure with a tunable optical Tamm state (OTS). Gunenthiran et al. [56] investigated the integration of fluorescent dye dendrimers (second-generation dendrimers) with the geometric characteristics of a porous scattering medium, nanoporous anodic aluminium oxide (NAA), to enhance random laser efficacy. Dendrimers contain fluorescent dye molecules and electrostatic interactions anchor them to the inner surface of the NAA platform, resulting in a solid-state composite structure. This research revealed that the NAA platform, characterized by low porosity and suitable thickness, when integrated with fluorescent molecules encapsulated by dendrimers, can facilitate high-quality random lasing. The optimized lasing platform generates highly polarized lasers (wavelength: 594 nm) with a superior gain product of 1588 au, a polarization mass of 0.86, and a lasing threshold of 0.05 mJ/pulse. The enhanced lasing platform markedly diminished the photobleaching effect and amplified the encapsulation effectiveness of the dendrimers by 2.5 times relative to conventional surfactants. These results indicate that the encapsulation of fluorescent molecules and the configuration of the scattering media significantly influence the development of random lasing platforms. These platforms provide innovative concepts for the application of optical and optoelectronic technology.

5.0 SUMMARY

This article analyzes and summarizes the fundamental principles underlying the synthesis of NAA, elucidates its synthetic mechanism, delves into the step-by-step synthetic process, and analyses numerous influencing elements in the oxidation of three common acidic solutions. A thorough examination of the results and conditions of these oxidizing acids revealed that the performance characteristics of the NAA structure, such as pore size and pore distance, are affected by factors such as the oxidizing acid type and concentration, oxidation time, current density, voltage, and temperature. The regulation of these parameters on pore properties such pore size, pore spacing, and structural stability is the main focus of a comparative study of anode conditions and their products under various

acidic environments. Furthermore, this study offers crucial theoretical direction for optimizing the NAA preparation procedure for particular uses. Researchers can further optimize the anodization method to attain improved material qualities by thoroughly comprehending the structure-effect relationship between synthesis circumstances and structural attributes. The technological developments in NAA synthesis covered in this article provide the groundwork for the creation of novel preparation techniques that have enormous potential for use in a variety of sectors, including biomedical engineering, energy storage, sensors, and optics.

ACKNOWLEDGEMENT

The authors would like to express their gratitude to Universiti Teknologi Malaysia for providing financial support for this research project under a UTM Fundamental Research Grant (Registration Proposal No: 22H86) and Professional Development Research University Fund (Registration Proposal No: 07E41). Additionally, the authors would like to acknowledge the Computational Solid Mechanics Lab, the Faculty of Mechanical Engineering, UTM, and Hebei Minzu Normal University, China for their continuous support.

REFERENCES

[1] H. Masuda, Highly Ordered Nanohole Arrays in Anodic Porous Alumina, in: Ordered Porous Nanostructures Appl., Springer-Verlag, New York, 2005: pp. 37–55. https://doi.org/10.1007/0-387-25193-6-3.
[2] J. Wook Yang, H. Ryeong Kwon, J. Ho Seo, S. Ryu, H. Won Jang, Nanoporous oxide electrodes for energy conversion and storage devices, RSC Appl. Interfaces 1 (2024) 11–42. https://doi.org/10.1039/D3LF00094J.
[3] D. Valero-Calvo, A. de la Escosura-Muñiz, Electroanalytical systems based on solid-state nanochannel arrays for the detection of biomarkers of interest in clinical diagnostics, TrAC Trends Anal. Chem. 172 (2024) 117568. https://doi.org/10.1016/j.trac.2024.117568.
[4] M. Wang, K. Chen, L. Xie, Y. Wu, X. Chen, N. Lv, F. Zhang, Y. Wang, B. Chen, Polarized emission of $Cs_3Cu_2I_5$ nanowires embedded in nanopores of an anodic aluminum oxide template, Opt. Lett. 49 (2024) 1349–1352. https://doi.org/10.1364/OL.515767.
[5] J. Lee, S. Shin, Y. Jiang, C. Jeong, H.A. Stone, C.-H. Choi, Oil-Impregnated Nanoporous Oxide Layer for Corrosion Protection with Self-Healing, Adv. Funct. Mater. 27 (2017) 1606040. https://doi.org/10.1002/adfm.201606040.
[6] C. Zhang, Z. Liu, C. Li, J. Cao, J.G. Buijnsters, Templated Synthesis of Diamond Nanopillar Arrays Using Porous Anodic Aluminium Oxide (AAO) Membranes, Nanomaterials 13 (2023) 888. https://doi.org/10.3390/nano13050888.
[7] H. Zhang, M. Zhou, H. Zhao, Y. Lei, Ordered nanostructures arrays fabricated by anodic aluminum oxide (AAO) template-directed methods for energy conversion, Nanotechnology 32 (2021) 502006. https://doi.org/10.1088/1361-6528/ac268b.
[8] M. Sener, O. Sisman, N. Kilinc, AAO-assisted nanoporous platinum films for hydrogen sensor application, Catalysts 13 (2023) 459. https://doi.org/10.3390/catal13030459.
[9] C.-A. Ku, C.-K. Chung, Advances in humidity nanosensors and their application: Review, Sensors 23 (2023) 2328. https://doi.org/10.3390/s23042328.
[10] J.V.D.S. Araujo, M. Milagre, I. Costa, A historical, statistical and electrochemical approach on the effect of microstructure in the anodizing of Al alloys: a review, Crit. Rev. Solid State Mater. Sci. (2023) 1–61. https://doi.org/10.1080/10408436.2023.2230250.
[11] P. Kapruwan, L.K. Acosta, J. Ferré-Borrull, L.F. Marsal, Optical platform to analyze a model drug-loading and releasing profile based on nanoporous anodic alumina gradient index filters, Nanomaterials 11 (2021) 730. https://doi.org/10.3390/nano11030730.
[12] E. Ducretet, Note sur un rhéotome liquide à direction constante, fondé sur une propriété nouvelle de l'aluminium, J. Phys. Théorique Appliquée 4 (1875) 84–85. https://doi.org/10.1051/jphystap:01875004008401.
[13] C. Pollak, German Patent: Elektrischer Flüssigkeitskondensator, 92564, 1897.
[14] S. Wernick, Electrolytic polishing and bright plating of metals, Redman, London, 1948.

[15] F. Keller, M.S. Hunter, D.L. Robinson, Structural Features of Oxide Coatings on Aluminum, J. Electrochem. Soc. 100 (1953) 411. https://doi.org/10.1149/1.2781142.
[16] The morphology and mechanism of formation of porous anodic films on aluminium, Proc. R. Soc. Lond. Math. Phys. Sci. (1970). https://doi.org/10.1098/rspa.1970.0129.
[17] J.P. O'Sullivan, J.A. Hockey, G.C. Wood, Infra-red spectroscopic study of anodic alumina films, Trans. Faraday Soc. 65 (1969) 535–541. https://doi.org/10.1039/TF9696500535.
[18] A. Baron-Wiechec, M. Burke, T. Hashimoto, H. Liu, P. Skeldon, G.E. Thompson, New Insights into Pore Initiation in Anodic Alumina, LATEST2, School of Materials, The University of Manchester, 2013.
[19] S. Toshihiko, K. Kyoko, Theories of anodized aluminum 100 Q&A., Arutopia, 27 (1997) 39–48.
[20] A.O. Araoyinbo, A.I. Azmi, C.M.R. Ghazali, A. Rahmat, K. Hussin, M.M.A. Abdullah, Nanoporous alumina fabrication: A short review, Nanosci. Nanotechnol.-Asia 7 (n.d.) 183–199. https://doi.org/10.2174/2210681206666161017120751.
[21] H. Masuda, K. Fukuda, Ordered Metal Nanohole Arrays Made by a Two-Step Replication of Honeycomb Structures of Anodic Alumina, Science 268 (1995) 1466–1468. https://doi.org/10.1126/science.268.5216.1466.
[22] G.D. Sulka, S. Stroobants, V. Moshchalkov, G. Borghs, J.-P. Celis, Synthesis of Well-Ordered Nanopores by Anodizing Aluminum Foils in Sulfuric Acid, J. Electrochem. Soc. 149 (2002) D97. https://doi.org/10.1149/1.1481527.
[23] W. Lee, R. Ji, C.A. Ross, U. Gösele, K. Nielsch, Wafer-Scale Ni Imprint Stamps for Porous Alumina Membranes Based on Interference Lithography, Small 2 (2006) 978–982. https://doi.org/10.1002/smll.200600100.
[24] A. Santos, C.S. Law, D.W.C. Lei, T. Pereira, D. Losic, Fine tuning of optical signals in nanoporous anodic alumina photonic crystals by apodized sinusoidal pulse anodisation, Nanoscale 8 (2016) 18360–18375. https://doi.org/10.1039/C6NR06796D.
[25] P. Csokan, Nucleation Mechanism in Oxide Formation During Anodic Oxidation of Aluminum, in: M.G. Fontana, R.W. Staehle (Eds.), Adv. Corros. Sci. Technol., Springer US, Boston, MA, 1980: pp. 239–356. https://doi.org/10.1007/978-1-4615-9065-1_4.
[26] J.M. Runge, The Metallurgy of Anodizing Aluminum: Connecting Science to Practice, 1st ed. 2018 edition, Springer, 2018.
[27] M.A. van Put, S.T. Abrahami, O. Elisseeva, J.M.M. de Kok, J.M.C. Mol, H. Terryn, Potentiodynamic anodizing of aluminum alloys in Cr(VI)-free electrolytes, Surf. Interface Anal. 48 (2016) 946–952. https://doi.org/10.1002/sia.5919.
[28] A.M. Abd-Elnaiem, A.M. Mebed, W.A. El-Said, M.A. Abdel-Rahim, Porous and mesh alumina formed by anodization of high purity aluminum films at low anodizing voltage, Thin Solid Films 570 (2014) 49–56. https://doi.org/10.1016/j.tsf.2014.08.046.
[29] M. Curioni, P. Skeldon, G.E. Thompson, J. Ferguson, Graded Anodic Film Morphologies for Sustainable Exploitation of Aluminium Alloys in Aerospace, Adv. Mater. Res. 38 (2008) 48–55. https://doi.org/10.4028/www.scientific.net/AMR.38.48.
[30] L. Zaraska, G. Sulka, J. Szeremeta, M. Jaskula, Porous anodic alumina formed by anodization of aluminum alloy (AA1050) and high purity aluminum, Electrochimica Acta 55 (2010) 4377–4386. https://doi.org/10.1016/j.electacta.2009.12.054.
[31] Z. Li, Y. Li, S. Li, J. Wu, X. Hu, Z. Ling, L. Jin, A Modified Quantitative Method for Regularity Evaluation of Porous AAO and Related Intrinsic Mechanisms, J. Electrochem. Soc. 165 (2018) E214. https://doi.org/10.1149/2.0841805jes.
[32] A.P. Leontiev, I.V. Roslyakov, K.S. Napolskii, Complex influence of temperature on oxalic acid anodizing of aluminium, Electrochimica Acta 319 (2019) 88–94. https://doi.org/10.1016/j.electacta.2019.06.111.
[33] P. Ramana Reddy, K.M. Ajith, N.K. Udayashankar, Effect of electrolyte concentration on morphological and photoluminescence properties of free standing porous anodic alumina membranes formed in oxalic acid, Mater. Sci. Semicond. Process. 106 (2020) 104755. https://doi.org/10.1016/j.mssp.2019.104755.
[34] F. Li, L. Zhang, R.M. Metzger, On the Growth of Highly Ordered Pores in Anodized Aluminum Oxide, Chem. Mater. 10 (1998) 2470–2480. https://doi.org/10.1021/cm980163a.
[35] W. Huang, M. Yu, S. Cao, L. Wu, X. Shen, Y. Song, Fabrication of highly ordered porous anodic alumina films in 0.75 M oxalic acid solution without using nanoimprinting, Mater. Res. Bull. 111 (2019) 24–33. https://doi.org/10.1016/j.materresbull.2018.11.002.
[36] A.P. Li, F. Müller, A. Birner, K. Nielsch, U. Gösele, Hexagonal pore arrays with a 50–420 nm interpore distance formed by self-organization in anodic alumina, J. Appl. Phys. 84 (1998) 6023–6026. https://doi.org/10.1063/1.368911.
[37] F.A. Bruera, G.R. Kramer, M.L. Vera, A.E. Ares, Low-Cost Nanostructured Coating of Anodic Aluminium Oxide Synthesized in Sulphuric Acid as Electrolyte, Coatings 11 (2021) 309. https://doi.org/10.3390/coatings11030309.
[38] H. Masuda, K. Yada, A. Osaka, Self-Ordering of Cell Configuration of Anodic Porous Alumina with Large-Size Pores in Phosphoric Acid Solution, Jpn. J. Appl. Phys. 37 (1998) L1340. https://doi.org/10.1143/JJAP.37.L1340.
[39] V. Sadasivan, C.P. Richter, L. Menon, P.F. Williams, Electrochemical self-assembly of porous alumina templates, AIChE J. 51 (2005) 649–655. https://doi.org/10.1002/aic.10332.

[40] A. Jagminienė, G. Valinčius, A. Riaukaitė, A. Jagminas, The influence of the alumina barrier-layer thickness on the subsequent AC growth of copper nanowires, J. Cryst. Growth 274 (2005) 622–631. https://doi.org/10.1016/j.jcrysgro.2004.10.021.
[41] P. Kapruwan, J. Ferré-Borrull, L.F. Marsal, Real-Time Monitoring of Doxorubicin Release from Hybrid Nanoporous Anodic Alumina Structures, Sensors 21 (2021) 7819. https://doi.org/10.3390/s21237819.
[42] T. Lednický, A. Bonyár, Large scale fabrication of ordered gold nanoparticle–epoxy surface nanocomposites and their application as label-free plasmonic DNA biosensors, ACS Appl. Mater. Interfaces 12 (2020) 4804–4814. https://doi.org/10.1021/acsami.9b20907.
[43] L. Pla, S. Santiago-Felipe, M.Á. Tormo-Mas, J. Pemán, F. Sancenón, E. Aznar, R. Martínez-Máñez, Aptamer-Capped nanoporous anodic alumina for *Staphylococcus aureus* detection, Sens. Actuators B Chem. 320 (2020) 128281. https://doi.org/10.1016/j.snb.2020.128281.
[44] H. Agbe, D.K. Sarkar, X.-G. Chen, N. Faucheux, G. Soucy, J.-L. Bernier, Silver–polymethylhydrosiloxane nanocomposite coating on anodized aluminum with superhydrophobic and antibacterial properties, ACS Appl. Bio Mater. 3 (2020) 4062–4073. https://doi.org/10.1021/acsabm.0c00159.
[45] Y. Liu, Y. Chen, Y. Guo, X. Wang, S. Ding, X. Sun, H. Wang, Y. Zhu, L. Jiang, Photo-controllable ion-gated metal–organic framework MIL-53 sub-nanochannels for efficient osmotic energy generation, ACS Nano 16 (2022) 16343–16352. https://doi.org/10.1021/acsnano.2c05498.
[46] W. Chen, Q. Zhang, Y. Qian, W. Xin, D. Hao, X. Zhao, C. Zhu, X.-Y. Kong, B. Lu, L. Jiang, L. Wen, Improved ion transport in hydrogel-based nanofluidics for osmotic energy conversion, ACS Cent. Sci. 6 (2020) 2097–2104. https://doi.org/10.1021/acscentsci.0c01054.
[47] Y. Fu, J. Yang, Y.S. Su, W. Du, Y.G. Ma, Daytime passive radiative cooler using porous alumina, Sol. Energy Mater. Sol. Cells 191 (2019) 50–54. https://doi.org/10.1016/j.solmat.2018.10.027.
[48] A. Díaz-Lobo, M. Martin-Gonzalez, Á. Morales-Sabio, C.V. Manzano, Suitability of anodic porous alumina as a passive radiative cooler: An in-depth study, ACS Appl. Opt. Mater. 2 (2024) 980–990. https://doi.org/10.1021/acsaom.3c00216.
[49] C.-A. Ku, C.-Y. Yu, C.-W. Hung, C.-K. Chung, Advances in the fabrication of nanoporous anodic aluminum oxide and its applications to sensors: A review, Nanomaterials 13 (2023) 2853. https://doi.org/10.3390/nano13212853.
[50] C.C. Yang, T.H. Liu, S.H. Chang, Relative humidity sensing properties of indium nitride compound with oxygen doping on silicon and AAO substrates, Mod. Phys. Lett. B 33 (2019) 1940044. https://doi.org/10.1142/S021798491940044X.
[51] C.K. Chung, O.K. Khor, C.J. Syu, S.W. Chen, Effect of oxalic acid concentration on the magnetically enhanced capacitance and resistance of AAO humidity sensor, Sens. Actuators B Chem. 210 (2015) 69–74. https://doi.org/10.1016/j.snb.2014.12.096.
[52] U. Malinovskis, A. Dutovs, R. Poplausks, D. Jevdokimovs, O. Graniel, M. Bechelany, I. Muiznieks, D. Erts, J. Prikulis, Visible photoluminescence of variable-length zinc oxide nanorods embedded in porous anodic alumina template for biosensor applications, Coatings 11 (2021) 756. https://doi.org/10.3390/coatings11070756.
[53] S. Gunenthiran, J. Wang, C.S. Law, A.D. Abell, Z.T. Alwahabi, A. Santos, Nanoporous anodic alumina photonic crystals for solid-state lasing systems: State-of-the-art and perspectives, J. Mater. Chem. C (2024). https://doi.org/10.1039/D4TC04166F.
[54] L. Liu, S.Y. Lim, C.S. Law, B. Jin, A.D. Abell, G. Ni, A. Santos, Engineering of broadband nanoporous semiconductor photonic crystals for visible-light-driven photocatalysis, ACS Appl. Mater. Interfaces 12 (2020) 57079–57092. https://doi.org/10.1021/acsami.0c16914.
[55] M. Li, C. Feng, L. Zhu, Y. Zhao, Fabrication of nanoporous anodized aluminum oxide based photonic crystals with multi-band responses in the vis-NIR region, Nanoscale (2024). https://doi.org/10.1039/D4NR04744C.
[56] S. Gunenthiran, C.S. Law, J. Wang, S.Y. Lim, A.D. Abell, Z.T. Alwahabi, A. Santos, Engineering of solid-state nanoporous laser through dendrimer-encapsulated fluorophores, ACS Appl. Mater. Interfaces 16 (2024) 15059–15072. https://doi.org/10.1021/acsami.4c00791.